ChemPubSoc Europe

DOI: 10.1002/cphc.201800139

CHEMPHYSCHEM Articles

Adsorption of 4,4′-Dithiodipyridine Axially Coordinated to Iron(II) Phthalocyanine on Au(111) as a New Strategy for Oxygen Reduction Electrocatalysis

Santiago Herrera,[a] Federico Tasca,[b] Federico J. Williams,[a] and Ernesto J. Calvo*[a]

The coordination of PySSPy to FePc was monitored by UV/Vis spectroscopy while the adsobed FePc, anchored by PyS–Au(111), was examined by in situ STM in 0.1 M $HClO_4$ and X-ray photoelectron spectroscopy (XPS). Rotating-disc-electrode (RDE) and linear-sweep-voltammetry (LSV) studies on the resulting FePc-modified Au(111) electrodes in an oxygen-saturated 0.1 M NaOH electrolyte exhibit excellent electrocatalytic properties for the oxygen reduction reaction (ORR), with a smaller overpotential than that observed for Au(111) with FePc deposited by direct adsorption from a benzene solution.

1. Introduction

It is well known that Iron(II) phthalocyanine (FePc) is an excellent electrocatalyst for the 4-electron oxygen reduction reaction (ORR) since the discovery of Jahnke and Schonborn in the 60′s.[1] Savy reported the highest activity for O_2 reduction in aqueous solutions;[2,3] subsequently van Veen and Visser[4] confirmed that FePc dispersed on high-area carbons is active for the O_2 reduction both in alkaline and acid solutions. The first step in the electrocatalysis is the formation of FePc-O_2 adduct with partial metal to O_2 charge transfer.[5] Quantum mechanical calculations predicted that the Fe(II)-O_2 would have an optimum electronic configuration for the subsequent activation and reduction of O_2[6] with charge transfer from the electron-rich Fe(II) centre to the O_2 π^* orbital. Zagal[7] described a mechanism for the O_2 reduction to water by soluble sulphonated FePc (FeTSPc) adsorbed on graphite electrodes. The key feature of this mechanism is the role of Fe(III)/Fe(II) redox couple, with ORR taking place at the reduced Fe(II)TSPc.

More recently, Tanaka et al.[8] reported Mössbauer, infrared spectroscopic and electrochemical studies of two μ-oxo iron phtalocyanine derivatives and FePc dispersed on carbon supports with redox processes in good agreement with redox potentials reported by Zecevic and Zagal.[7,9] Self-assembled 4-mercaptopyridine (4-MPy) on Au(111) is an excellent axial ligand to anchor transition metal complexes as shown with $Ru(CN)_5$ Py,[10] $PtCl_4$[2,11] and $PdCl_4$.[2,12] In particular, self- assembled monolayers of 4-mercaptopyridine adsorbed on Au(111) from ethanol solutions with further coordination of FePc have been reported.[13–15] It should be noted that adsorption of 4MPy from ethanol solutions leads to decomposition and formation of atomic sulphur on the surface.[16–18]

In the present work we have followed a different strategy, namely the dithiol 4,4′-dithiodipyridine in benzene solvent, which is a bad axial ligand for the Fe centre, was coordinated to FePc in a 1:1 molar ratio to avoid thiol excess which would otherwise easily self-assemble on the Au(111) surface. Scheme 1 shows a schematic representation of the reaction path used to form the electroactive self-assembled monolayer.

In a first step, a benzene saturated solution of FePc was allowed to react with PySSPy which axially coordinates the Fe(II) site in FePc. Oxygen was removed by bubbling argon in order to prevent its coordination to the d_{z2} orbital of the macrocycle metal centre. The second step consists in the formation of the self-assembled monolayer by immersion of the Au(111) substrate in the reaction solution for short times. As depicted in scheme I, when the FePc-PySSPy reaches the gold surface, the S–S bond breaks and 4-mercaptopyridine self-assembles.[19,20] This methodology allows control not only of the ratio between FePc and PySSPy but also the amount of catalytic centres attached to the surface by simply controlling the adsorption time. By a careful characterization of the Au modified surfaces using X-Ray photoelectron spectroscopy we have described the molecular nature of the iron phthalocyanine tethered to Au by coordinated mercapto pyridine as confirmed by STM. The modified surface enhances the 4-electron oxygen reduction reaction by decreasing the overpotential.

2. Results and Discussion

UV/Vis spectra of FePc saturated in benzene were recorded prior to the reaction (Figure 1 – black line). Two absorption peaks can be seen for the Q-band region with a low absorbance despite the high molar absorptivity of FePc. When a single drop of pyridine was added to the solution, a completely different spectra was obtained (Figure 1 – green line). The absorbance at

[a] S. Herrera, Dr. F. J. Williams, Prof. E. J. Calvo
Department of Inorganic Chemistry, Analytical and Chemical Physics, INQUIMAE-CONICET
Facultad de Ciencias Exactas y Naturales, Universidad de Buenos Aires
Ciudad Universitaria, Pabellón 2, Buenos Aires C1428EHA, Argentina
E-mail: calvo@qi.fcen.uba.ar

[b] Dr. F. Tasca
Department of Chemistry Materials
Facultad de Química y Biología, Universidad de Santiago de Chile
Av. Libertador Bernardo O'Higgins 3363, Santiago, Chile

Supporting information for this article is available on the WWW under https://doi.org/10.1002/cphc.201800139

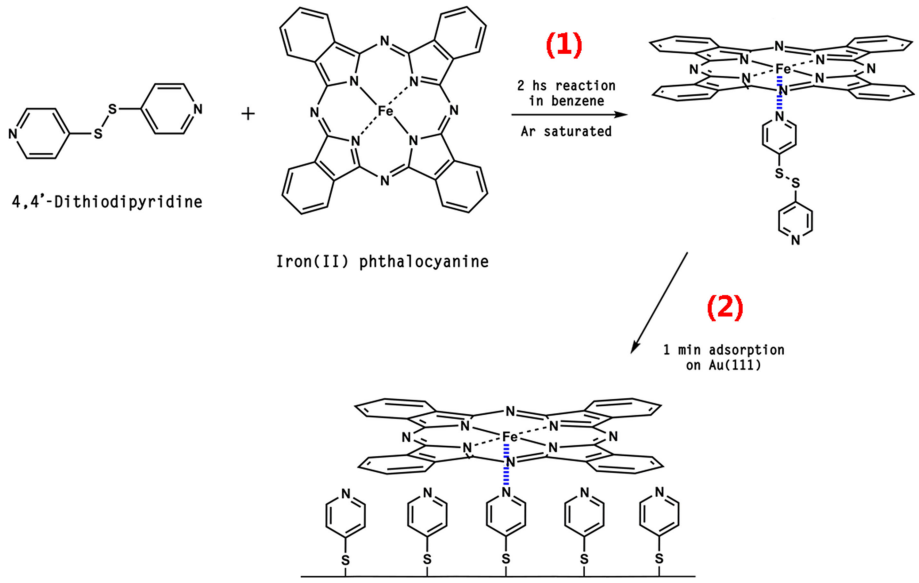

Scheme 1. Self-assembled monolayer formation scheme. On the first step, the PySSPy reacts in solution with FePc to give the axially coordinated FePc complex. After two hours of reaction, the self-assembly is established by immersing the gold single crystal for 1 min into the reaction solution.

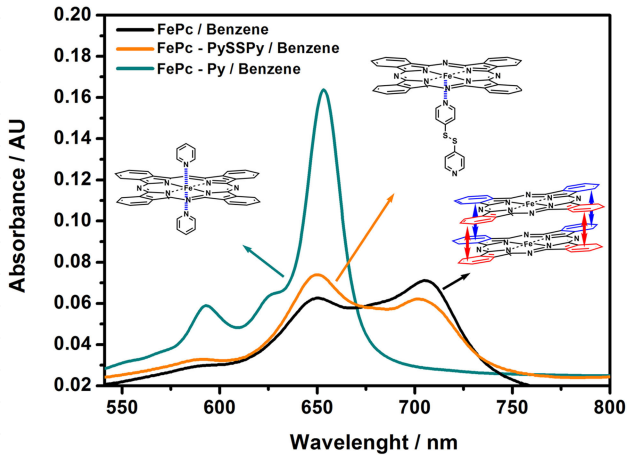

Figure 1. UV/Vis spectra of: FePc in benzene (black line); FePc in benzene with excess of pyridine (green line); and FePc/PySSPy in benzene after two hours of reaction (orange line). The insets show schematics of molecules in solution.

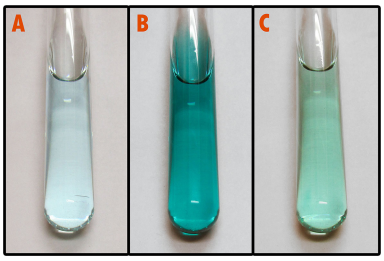

Figure 2. Test tubes indicating the colours and their intensities according to the different coordination of FePc: A) FePc in benzene; B) FePc in benzene with excess of pyridine; and C) FePc/PySSPy (1:1) in benzene after two hours of reaction.

650 nm increases while the 705 nm band disappears completely. Also the colour of the solution changes rapidly after the addition of pyridine as can be seen in the pictures depicted on Figure 2A–B. Under the experimental conditions, the 650 nm absorption peak corresponds to the single FePc monomer Q-band and the peak at 705 nm to FePc forming pairs of molecules stabilized by π-π stacking. After adding pyridine which strongly binds to the iron centre[21] as an axial ligand, the dimers break and the 705 nm peak disappears while the monomeric phtalocyanine solubility increases and only the FePc-monomer Q-band absorption peak is observed. We rationalize the low absorbance of the solution assuming that initially the solution is saturated with FePc with extremely low solubility in benzene because of the low interaction between the FePc and benzene.

The reaction between PySSPy and FePc has been followed by monitoring the changes in the UV-Vis spectrum: the total absorbance slowly reaches a steady value after 2 hours. The solution colour changes from light blue to green (Figure 2-C) and the ratio of the absorption bands at 650 nm and 705 nm change slightly showing that after 2 hours of reaction the coordination of pyridine to the Fe atom has taken place. Some dimer is still present as seen in Figure 1 (orange line). In this experiment the concentration of the PySSPy was fixed to 1.75 μM while the total concentration of FePc in the saturated benzene solution was estimated to be 2 μM by UV-Vis experiments. For larger concentration of dithiol, no electrochemical oxygen reduction can be observed since the electrode surface is completely covered by a passivating thiol monolayer (STM).

The FePc and FePc/PySSPy solutions in benzene were used separately to modify the Au(111) crystal by immersion for short periods of time. After the direct adsorption of FePc on Au(111), in situ STM reveals that some ordered FePc domains were formed on isolated areas (Figure 3-B). These compact domains are surrounded by large areas where no order was found resulting in a heterogeneous FePc deposit. Similar results were

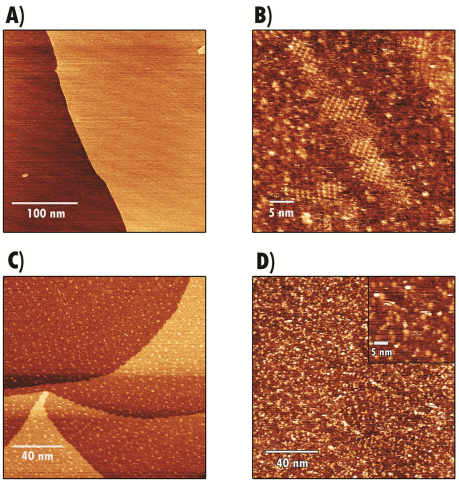

Figure 3. In situ STM images of: A) Clean Au(111) substrate; B) FePc-modified electrode (5 min adsorption); C) FePc/PySSPy-modified electrode (3 seconds adsorption); and D) FePc/PySSPy-modified electrode (1 min adsorption). $E_{sub} = 0.3$ V. STM sample bias potential and set point currents fixed to 300 mV and 400 pA, respectively. $HClO_4$ 0.1 M was used as electrolyte.

reported by Gu et. al. using DMF saturated FePc solutions [16]. The distance between adjacent molecules was estimated 1.4± 0.1 nm in accordance with the literature [16].

The images also reveal that in some cases the FePc forms double layers, possibly by adsorption of dimers or by co-adsorption of a second molecular layer. If the Au substrate potential is shifted from open circuit potential down to the hydrogen evolution region, no changes in the adsorbed FePc features could be detected.

The self-assembly of the catalyst on Au(111) was performed by immersion of the Au(111) single crystal in a benzene solution of FePc-PySSPy during different times in order to optimize the catalyst loading and thus the electro catalytic activity. Previous studies have shown that 4-mercaptopyridine or PySSPy suffer from side reactions at the Au surface for long incubation times depending on the solvent.[17] In ethanol solutions, the self-assembled monolayer can be oxidized after a few seconds of immersion and results in a thick layer of decomposition products.[16] Using water as solvent, decomposition of the self-assembled monolayer can take place after 5 minutes of immersion. In order to prevent the oxidation of the thiol group and to avoid side reactions during the adsorption step, the immersion time was limited to less than 3 minutes.

Figures 3C and D show in-situ STM images of Au(111) after adsorption of FePc-PySSPy during 3 seconds and 1 minute respectively. At short adsorption time (3 seconds) iron phthalocyanine is coordinated to pyridines over the $(22\times\sqrt{3})$ gold reconstruction resulting in an homogeneous deposit forming straight lines separated by 6 nm (Figure 3C) unlike FePc directly adsorbed on Au(111) (Figure 3 B) with disordered molecular patches.

Estimation of surface coverage from analysis of STM images gives 2.36×1012 molecules cm-2. A closer look into the STM images shows that the region between the bright spots is covered by thiol molecules as they show the same feature than the images obtained by direct thiol adsorption (Figures S1 and S2). This means that the free PySSPy molecules adsorb randomly on the surface but the FePc-PySSPy follows the reconstruction lines driven by some specific interaction with the substrate. Figure 3D shows that after 1 min of adsorption of FePc-PySSPy the loading of the catalyst increases up to 9.8× 1012 molecules cm-2, more than four times the coverage obtained by 3 sec of adsorption. The deposit is also fully homogeneous, no preferential adsorption sites are observed and a dense deposit of catalyst is obtained. If the potential of the substrate is shifted in negative direction, the deposit remains stable and no desorption is observed between the open circuit potential and the hydrogen evolution potential (0 V in $HClO_4$ 0.1 M).

Figure 4 depicts the C 1s, N 1s, S 2p and Fe 2p3/2 XPS spectra before and after exposing the Au(111) surface to a 1:1 FePc:PySSPy benzene solution for 1 minute. Initially the Au (111) surface does not contain any XPS detectable traces of C, N, S or Fe indicating that the crystal is clean. Broad XPS spectra show only Au related signals. After adsorption of the FePc/PySSPy on Au(111) surface C, N, S and Fe XPS signals are observed in agreement with the chemical composition of the monolayer. Also the Au 4f peak is attenuated confirming the presence of the monolayer. The C 1s spectrum shown in Figure 4a and corresponding to the FePc-PySSPy functionalized surface has contributions around 284.2 eV due to the benzene carbons in FePc, at 285.2 eV due to pyrrole carbons in FePc with an additional contribution of carbons in pyridine mole-

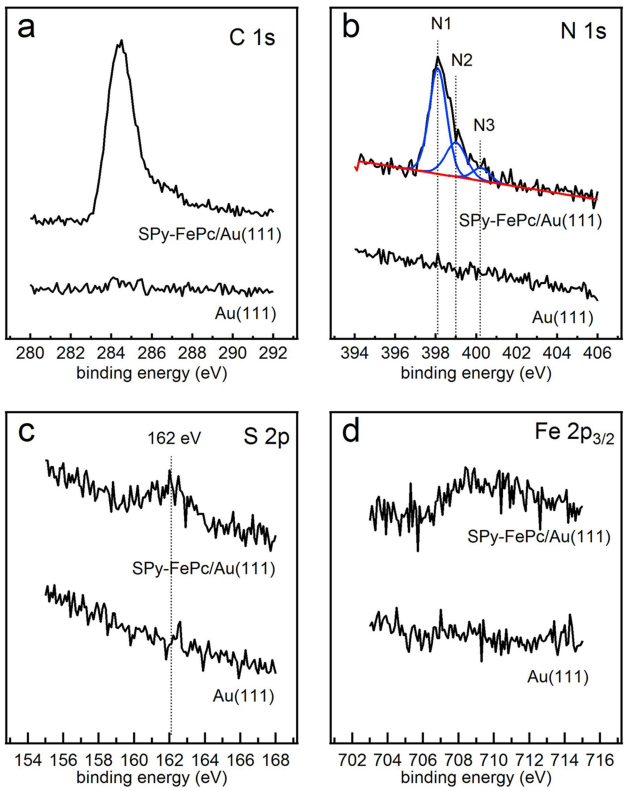

Figure 4. C 1s, N 1s, S 2p, and Fe $2p_{3/2}$ XPS spectra before and after exposing the Au(111) surface to a FePc-PySSPy benzene solution for 1 minute.

cules and at 286.2 eV due to carbon atoms in the pyridine molecules that are attached to the FePc.[21] These signals overlap with shake up satellites at approximately 285 and 287 eV making the quantitative analysis of the region difficult. The N 1s XPS spectrum in Figure 4b that corresponds to the FePc/PySSPy functionalized Au(111) surface has three clear contributions at 398.1 eV (N1) due to the nitrogen atoms in the FePc rings, at 399 eV (N2) due to the uncoordinated nitrogen atoms in the pyridine molecules and at 400.2 eV (N3) due to the FePc coordinated nitrogen atoms in the pyridine molecules. Here we should note that this assignment is based upon the detailed XPS study of the interaction of pyridine molecules with a single layer of FePc over Au(111) carried out by Schnadt and co-workers.[21] The N3:N1 integrated intensity ratio is 8:1 indicating that all the surface FePc molecules (8 N atoms per molecule) are coordinated to Pyridine molecules (1 N atom per molecule). Furthermore the N2:N3 ratio is 3.1:1 indicating that there are surface Pyridine molecules which are not coordinated to FePc.

The S 2p XPS spectrum in Figure 4c that corresponds to the FePc-PySSPy/Au(111) surface has a single broad contribution at around 162 eV confirming that all the PySSPy molecules are bound covalently to the surface via a thiolate Au–S bond as expected.[22] The observed (N2+N3):S ratio is 1.5:1 which is greater than the expected 1:1 ratio due to the attenuation of the S signal caused by the rest of the Pyridine backbone and the overlying FePc molecules.

The Fe $2p_{3/2}$ spectrum corresponding to the FePc-PySSpy/Au(111) surface shown in Figure 4d has a broad contribution centered at approximately 709 eV due to the Fe centers in the FePc molecules. The observed N3:Fe ratio is 1.1:1 in excellent agreement with the expected 1:1 ratio as all FePc molecules are bound to the surface via a pyridine coordinating molecule.

Figure 5A depicts O_2 reduction polarization curves obtained using an Au disc electrode modified with FePc coordinated to PySSPy in alkaline solution at different rotation frequency with an onset potential at −67 mV. Koutecky-Levich plots (Figure 5B) recorded at different potentials show parallel straight lines the slopes of which yield n = 3.6 electrons per O_2 molecule by using $C_{O2} = 1.18\times10^{-6}$ mol cm^{-3}, $D_{O2} = 1.9\times10^{-5}$ cm^2 s^{-1} and $\nu = 8.93\times10^{-3}$ cm^2 s^{-1}. This result indicates that the reduction of O_2 undergoes predominantly a 4 electron mechanism catalyzed by the adsorbed FePc–Py complex.

The ORR on Au in alkaline solutions is a well known 2-electron process[23] while on FePc is a 4-electron process[7] therefore as seen in Figure 3 combination of patches covered by FePc and areas of bare Au result in $2 \le n_{eff} \le 4$. Furthermore, in Supporting Information Figures S4 and S5 depict polarization curves and Koutecky-Levich plots for ORR on bare Au and partly covered Au by FePc with $n_{eff} = 2.05$ and 3.6 respectively.

Figure 6 shows RDE polarization curves for the clean Au surface (blue line), FePc directly adsorbed on Au (green line), FePc/ PySSPy adsorbed on Au for 3 seconcs (brown line) and 1 min (orange line). Clearly, the ORR polarization curves show that the onset potential shifts to positive values when Au is coated with FePc and FePc-PySSPy. The ORR on bare Au has a more negative onset potential and the convective-diffusion

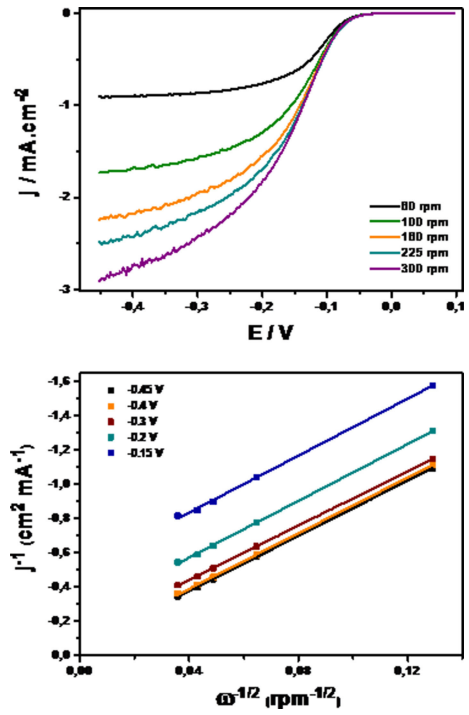

Figure 5. ORR rotating disc electrode electrochemistry of an FePc-PySSPy-modified electrode (t_{mod} = 1 min): A) Polarization curves at different rotating speeds; oxygen-saturated 0.1 M KOH, scan rate: 5 mV s^{-1}. B) Koutecky-Levich plots at different potentials.

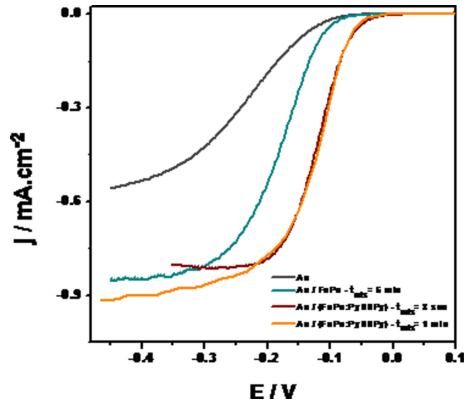

Figure 6. RDE polarization curves for different Au surfaces: Clean Au (blue line); FePc-modified electrode for 5 min (green line); FePc-PySSPy-modified electrode for 3 sec (brown line) and FePc-PySSPy-modified electrode for 1 min (orange line). Oxygen-saturated 0.1 M KOH, scan rate: 5 mV s^{-1}, rotation speed: 60 rpm.

limiting current corresponds to n = 2.[23] The ORR on FePc directly ad-sorbed on Au exhibited an onset potential of −110 mV.

The FePc adsorbed on Au(111) leaves uncovered Au patches on the surface and therefore the ORR proceeds via two parallel pathways: 2- and 4-electron reduction at bare Au and at the FePc respectively.

Furthermore, as shown in Figure S6, the reduction of O_2 by FePc is tuned to the redox potential of the Fe(III)/Fe(II) couple in aqueous solution and Fe(II) is the active site for O_2

reduction.[7] Anchoring a pyridine on the axial position of the Fe center produces a positive shift in the ORR onset potential of about +40 mV indicating a stabilization of the Fe(II) species and thus decreasing the overpotential of the Fe(III)/Fe(II) site.[15,24] Lever has shown that the redox potential for Fe(III)/Fe(II) in non-aqueous solvents exhibits a maximum value (positive values) in pyridine as a solvent, and minimum value (negative value) in dichloromethane.[25] An increment of the solvent donor number favors the stabilization of Fe(II) in the macrocycle. In particular pyridine not only has a high donor number but also forms a strong bond with the Fe center due to σ-bonding and π back bonding which enhances the covalent interaction.[26]

We should finally note that increasing the catalyst loading by varying the adsorption time from 3 seconds to 1 minute results in the same ORR onset potential (Figure 6, brown and orange lines).

This implies that the thermodynamic redox potential for Fe(III)/Fe(II) is fixed by the chemical identity of the molecules and not by the surface density. On the contrary, the limiting ORR currents observed at high overpotentials are slightly greater for electrodes with high surface density (1 min adsorption).

According to the Levich equation the convective-diffusion limiting current depends on 3 factors: O_2 analytical concentration, dif-fusion coefficient, and effective number of electrons, n_{eff} ($2 \leq n_{eff} \leq 4$). Thus, if the FePc catalyzes a 4 electron reaction, the bare Au patches would contribute with 2 electron path.[27–29] and n_{eff} will depend on the coverage by FePc consistent with the observation also seen in stationary electrodes (Figure S3).

3. Conclusions

Adsorption of 4,4′-dithiodipyridine axially coordinated to Iron phtalocyanine on Au(111) single crystal electrode with cleavage of the S–S bond and formation of Au–S bond results in a stable and reproducible electrode modification with FePc-PyS–Au.

The modified surface was characterized by UV-visible spectroscopy, *in situ* electrochemical STM in 0.1 M $HClO_4$ and by X-ray photoelectron spectroscopy (XPS). Rotating disc electrode (RDE) and linear sweep voltammetry (LSV) of the resulting FePc-PySSPy modified Au(111) electrode in oxygen saturated 0.1 M KOH electrolyte exhibits excellent electro-catalysis for the oxygen reduction reaction (ORR) with a 4-electron pathway.

The new strategy results in a reduction of the ORR overpotential as compared to direct adsorption of FePc and increase of the number of electrons per oxygen molecule.

Experimental Section

Materials

Benzene (Merck), Iron(II) phthalocyanine (FePc), 4,4′-Dithiodipyridine (PySSPy) and Potassium Hydroxide (Sigma-Aldrich) were used as received without further purification.

FePc/PySSPy Axial Coordination

A saturated solution of FePc in benzene (50 mL) was deoxygenated by bubbling argon and 875 μL of a 0.1 mM PySSPy solution in benzene were added.

FePc/PySSPy Self-Assembly

After two hours of reaction between FePc and PySSPy in benzene, Au electrodes were immersed in the solution for 3 seconds or 1 minute depending on the experiment. For ECSTM and XPS studies an Au(111) sample was used, while a polycrystalline Au electrode was employed for RDE and LSV experiments. After self-assembly, the electrodes were washed with pure benzene and then with Milli-Q water to remove any excess of reactants.

FePc Self-Adsorption

The clean substrates were immersed in a saturated FePc benzene solution for 5 minutes and further washed.

Electrochemical Experiments

Electrochemical measurements were carried out with an Autolab V 30 system (Eco Chemie, Utrecht, The Netherlands) controlled by NOVA 1.11 Software and a rotation controller. The 0.196 cm^2 Au disc electrodes were embedded in Kel-F sheaths. RDE and LSV experiments were performed using a three-electrode glass cell with a Pt counter electrode and an Ag/AgCl 3 M KCl reference electrode. Potentials herein are quoted with respect to this reference. All experiments were carried out at room temperature ($20 \pm 2\,^{\circ}C$). Before each experiment the working Au electrode was polished with 3 M® 1200 grit emery followed by: (i) 5, 1, 0.3 and 0.05 μm alumina (Buehler) each followed by 5 minutes sonication in isopropanol-water solution to remove excess alumina. Electrochemical cleaning was carried out before adsorption by cycling the working electrode potential from 0.4 V to 1.5 V in an argon saturated 0.5 M $HClO_4$ aqueous solution until the typical cyclic voltammetry of clean gold was obtained. An O_2 saturated 0.1 M KOH aqueous solution was employed for the ORR studies. O_2 reduction polarization curves were recorded at 5 $mV\,s^{-1}$ above −0.5 V to avoid reductive desorption of the self-assembled monolayer (Figure S4).

UV/Vis Absorption Spectroscopy Measurements

UV-Vis spectra were recorded on a Shimadzu UV-1603. At different time intervals, aliquots of the reaction solution were taken and placed directly into a quartz cuvette for spectroscopic analysis.

X-ray Photoelectron Spectroscopy Measurements

X-ray photoelectron spectroscopy (XPS) measurements were conducted in an ultrahigh vacuum (UHV) chamber with a base pressure below 5×10^{-10} mbar, using a 150 mm hemispherical SPECS electron energy analyser and a monochromatic Al Kα X-ray source. Binding energies reported in this work are referenced to the Fermi edge of Au(111) at EB = 0 eV. The Au(111) single crystal was cleaned by repetitive cycles of argon sputtering and annealing. It was then exposed to a FePc:PySSPy 1:1 benzene solution using the liquid reactor attached to the UHV system previously described.[30] Finally the Au(111) surface modified with phthalocyanine was rinsed with benzene and milliQ® water before transferring it back to the analysis chamber to acquire the XPS spectra. Atomic ratios were

calculated from the integrated intensities of core levels after instrumental and photoionization cross sect ion corrections.

Electrochemical Scanning Tunnelling Microscopy

A Scanning Probe Microscope AFM-STM 5500 (Agilent Technologies ®) with four-electrode bi-potentiostat for the independent control of substrate and tip potentials with respect to the reference electrode in the electrolyte was used for in situ electrochemical scanning tunnelling microscopy (ECSTM) measurements. The gold single-crystal electrode used in these measurements was a solid cylinder (MaTeck, Germany, 1 cm diameter, polished down to 0.03 μm) with one of its ends oriented better than 1° along the (111) plane. Prior to each experiment, the Au crystal was annealed for 5 min in a hydrogen flame, allowed to cool in air. Tungsten tips were prepared by etching in 2 M KOH and then cleaned with concentrated hydrofluoric acid, water and acetone. To minimize Faradaic currents the tips were isolated with nail paint and dried overnight. The custom-made three-electrode PTFE cell was used with two Pt wires used as counter and pseudo-reference electrodes respectively and 0.1 M $HClO_4$ aqueous solution was used as electrolyte.

Acknowledgements

The authors acknowledge financial support from CONICET, ANCPCyT and the University of Buenos Aires. F.T. thanks the Teaching Program of Montevideo Group of Universities, AUGM for a visit grant at University of Buenos Aires, Fondecyt 11130167 and "Proyectos Basales".

Conflict of Interest

The authors declare no conflict of interest.

Keywords: electrocatalysis · oxygen reduction reaction · phthalocyanines · scanning tunnelling microscopy · X-ray spectroscopy

[1] H. Jahnke, M. Schönborn, G. Zimmermann, *Top. Curr. Chem.* **1976**, *61*, 133–181.
[2] M. Savy, P. Andro, C. Bernard, G. Magner, *Electrochim. Acta* **1973**, *18*, 191–197.
[3] M. Savy, C. Bernard, G. Magner, *Electrochim. Acta* **1975**, *20*, 383–391.
[4] J. A. R. van Veen, C. Visser, *Electrochim. Acta* **1979**, *24*, 921–928.
[5] F. Beck, *J. Appl. Electrochem.* **1977**, *7*, 239–245.
[6] J. E. Newton, M. B. Hall, *Inorg. Chem.* **1984**, *23*, 4627–4632.
[7] J. Zagal, P. Bindra, E. Yeager, *J. Electrochem. Soc.* **1980**, *127*, 1506–1517.
[8] A. A. Tanaka, C. Fierro, D. Scherson, E. B. Yeager, *J. Phys. Chem.* **1987**, *91*, 3799–3807.
[9] S. Zecevic, B. Simic-Glavaski, E. Yeager, A. B. P. Lever, P. C. Minor, *J. Electroanal. Chem.* **1985**, *196*, 339–358.
[10] I. C. N. Diógenes, F. C. Nart, M. L. A. Temperini, Í. d. S. Moreira, *Inorg. Chem.* **2001**, *40*, 4884–4889.
[11] M. Manolova, V. Ivanova, D. M. Kolb, H. G. Boyen, P. Ziemann, M. Büttner, A. Romanyuk, P. Oelhafen, *Surf. Sci.* **2005**, *590*, 146–153.
[12] V. Ivanova, T. Baunach, D. M. Kolb, *Electrochim. Acta* **2005**, *50*, 4283–4288.
[13] K. I. Ozoemena, T. Nyokong, *J. Electroanal. Chem.* **2005**, *579*, 283–289.
[14] I. Ponce, J. F. Silva, R. Oñate, M. C. Rezende, M. A. Paez, J. H. Zagal, J. Pavez, F. Mendizabal, S. Miranda-Rojas, A. Muñoz-Castro, R. Arratia-Pérez, *J. Phys. Chem. C* **2012**, *116*, 15329–15341.
[15] J. F. Silva, J. Pavez, C. P. Silva, J. H. Zagal, *Electrochim. Acta* **2013**, *114*, 7–13.
[16] K. Umemura, K. Fujita, T. Ishida, M. Hara, H. Sasabe, W. Knoll, *Japanese Journal of Applied Physics, Part 1: Regular Papers and Short Notes and Review Papers.* **1998**, *37*, 3620–3625.
[17] S. Yoshimoto, M. Yoshida, S. I. Kobayashi, S. Nozute, T. Miyawaki, Y. Hashimoto, I. Taniguchi, *J. Electroanal. Chem.* **1999**, *473*, 85–92.
[18] E. A. Ramírez, E. Cortés, A. A. Rubert, P. Carro, G. Benítez, M. E. Vela, R. C. Salvarezza, *Langmuir.* **2012**, *28*, 6839–6847.
[19] Zhou, T. Baunach, V. Ivanova, D. M. Kolb, *Langmuir.* **2004**, *20*, 4590–4595.
[20] B. Koslowski, A. Tschetschetkin, N. Maurer, P. Ziemann, J. Kučera, A. Groß, *J. Phys. Chem. C* **2013**, *117*, 20060–20067.
[21] C. Isvoranu, B. Wang, E. Ataman, K. Schulte, J. Knudsen, J. N. Andersen, M.-L. Bocquet, J. Schnadt, *J. Phys. Chem. C* **2011**, *115*, 20201–20208.
[22] C. Vericat, M. E. Vela, G. Corthey, E. Pensa, E. Cortes, M. H. Fonticelli, F. Ibanez, G. E. Benitez, P. Carro, R. C. Salvarezza, *RSC Adv.* **2014**, *4*, 27730–27754.
[23] R. W. Zurilla, R. K. Sen, E. Yeager, *J. Electrochem. Soc.* **1978**, *125*, 1103–1109.
[24] R. Cao, R. Thapa, H. Kim, X. Xu, M. Gyu Kim, Q. Li, N. Park, M. Liu, J. Cho, *Nat. Commun.* **2013**, *4*, 2076.
[25] E. R. Milaeva, G. Speier, A. B. Lever, Y.U.N.Y.D. o. CHEMISTRY in The Redox Chemistry of Metallophthalocyanines in Solution, Vol. (Ed. Eds.: Editor), Defense Technical Information Center, City, **1992**.
[26] A. B. P. Lever, P. C. Minor, *Adv. Mol. Relax. Interact. Processes* **1980**, *18*, 115–126.
[27] I. Ponce, J. F. Silva, R. Oñate, M. C. Rezende, M. A. Páez, J. Pavez, J. H. Zagal, *Electrochem. Commun.* **2011**, *13*, 1182–1185.
[28] Z. H. Cheng, L. Gao, Z. T. Deng, Q. Liu, N. Jiang, X. Lin, X. B. He, S. X. Du, H. J. Gao, *J. Phys. Chem. C* **2007**, *111*, 2656–2660.
[29] Z. H. Cheng, L. Gao, Z. T. Deng, N. Jiang, Q. Liu, D. X. Shi, S. X. Du, H. M. Guo, H. J. Gao, *J. Phys. Chem. C* **2007**, *111*, 9240–9244.
[30] E. de la Llave, S. E. Herrera, L. P. Méndez De Leo, F. J. Williams, *J. Phys. Chem. C* **2014**, *118*, 21420–21427.

Manuscript received: February 12, 2018
Version of record online: May 7, 2018